Electrocatalytic Reduction of Nitrite and Nitrosyl by Iron(III) Protoporphyrin IX Dimethyl Ester Immobilized in an Electropolymerized Film

Janet N. Younathan,† Karen S. Wood, and Thomas J. Meyer*

Department of Chemistry, The University of North Carolina, Chapel Hill, North Carolina 27599-3290

Received August 6, 1991

Thin polymeric films formed by anodic electropolymerization of an iron(III) protoporphyrin IX dimethyl ester complex, [Fe^{III}(PP)Cl], on glassy-carbon or optically transparent SnO_2 electrodes are effective catalysts for the electroreduction of $HONO/NO_2^-$ or NO to N_2O, N_2, NH_2OH, and NH_3. The yield of N_2 is enhanced in the compact environment of the redox polymer relative to that for comparable monomeric metalloporphyrins in homogeneous solution.

Introduction

The biochemical reduction of nitrite to ammonia that occurs in green plants is a six-electron, seven-proton process catalyzed by the nitrite reductase enzymes (eq 1).[1-11] These enzymes are

$$NO_2^- + 7H^+ + 6e^- \rightarrow NH_3 + 2H_2O \qquad (1)$$

complex proteins consisting of an iron–sulfur unit and an iron isobacteriochlorin or siroheme.[1-6,8-10] Biochemical studies indicate that the iron–sulfur unit accepts electrons from reduced ferredoxin, subsequently transferring them to siroheme, the binding site for the nitrite anion.[1,5,7,11]

The biological catalysts have been mimicked synthetically by using accessible isobacteriochlorins.[12-14] In addition, simple transition metal complexes have been employed as enzymatic models for nitrite reduction. Studies utilizing polypyridyl complexes of ruthenium and osmium have demonstrated the facile interconversion of bound nitrite and nitrosyl[15] and the chemical and electrochemical reduction of bound nitrosyl to coordinated ammonia.[16-22] Electrochemical investigations allowed detection of intermediate products as coordinated ligands and provided support for a mechanism invoking a series of one-electron reductions at NO.[19-22]

While the osmium and ruthenium complexes do not serve as catalysts for nitrite reduction because of strong ligand binding, water-soluble iron porphyrins accelerate reduction of nitrite in acidic solution producing a variety of products including N_2O, N_2, NH_3OH^+, and NH_4^+.[19,23-25] Investigations of the spectroscopic and electrochemical properties of iron porphyrins in the presence of nitrite reveal that key intermediates in the metalloporphyrin-mediated reduction of nitrite are iron nitrosyl complexes that are analogous to those observed with osmium and ruthenium complexes. In acidic, aqueous solution where the proton demands of the reaction are met, subsequent reduction to bound ammonia can occur.

One of our interests in this area is in the development of catalysts capable of mediating multiple electron-transfer reactions which model the activity of the biological systems. An elegant example of a multielectron nitrite reduction catalyst has already appeared in the work of Toth and Anson,[26] who demonstrated that iron-substituted heteropolytungstates are robust catalysts for the conversion of nitrite to ammonia. We have transferred the reactivity of an iron porphyrin to the electrode–solution interface, incorporating the porphyrin into a thin polymeric film by oxidative electropolymerization. The polymeric structure may possess some of the properties of the biological catalyst, since enzymatic modeling reveals that the binding site in nitrite reductase is embedded in a nonaqueous environment similar to an aprotic medium.[27] The porphyrin complex chosen for the film experiments, an iron(III) protoporphyrin IX dimethyl ester complex (**1**, Fe^{III}(PP)Cl; see Figure 1), has well-characterized redox properties both as a monomer in homogeneous solution[28] and as an insoluble polymeric film supported on an electrode surface.[28-30]

† NIH Postdoctoral Fellow, 1987–88. Present address: Eastman Kodak Co., Rochester, NY 14650-2102.

(1) Losada, M. *J. Mol. Catal.* **1975/76**, *1*, 245.
(2) Candau, P.; Manzano, C.; Losada, M. *Nature (London)* **1976**, *262*, 715.
(3) Losada, M. *Bioelectrochem. Bioenerg.* **1979**, *6*, 205.
(4) Guerrero, M. G.; Vega, J. M.; Losada, M. *Annu. Rev. Plant Physiol.* **1981**, *32*, 169.
(5) Murphy, M. J.; Siegel, L. M.; Tove, S. R.; Kamin, H. *Proc. Natl. Acad. Sci. U.S.A.* **1974**, *71*, 612.
(6) Lancaster, J. R.; Vega, J. M.; Kamin, H.; Orme-Johnson, N. R.; Orme-Johnson, W. H.; Krueger, R. J.; Siegel, L. M. *J. Biol. Chem.* **1979**, *254*, 1268.
(7) Pivalle, L. S.; Privalle, C. T.; Leonardy, N. J.; Kamin, H. *J. Biol. Chem.* **1985**, *260*, 14344.
(8) Averill, B. A.; Orme-Johnson, W. H. In *Metal Ions in Biological Systems*; Sigel, H., Ed.; Marcel Dekker: New York, 1978; Vol. 7, Chapter 4.
(9) Prodouz, K. N.; Garrett, R. H. *J. Biol. Chem.* **1981**, *256*, 9711.
(10) Romero, L. C.; Borrero, J. A.; Galvan, F.; Vega, J. M. *J. Mol. Catal.* **1989**, *57*, 259.
(11) Mikami, B.; Ida, S. *J. Biochem. (Tokyo)* **1989**, *105*, 47.
(12) Chang, C. K.; Hanson, L. K.; Richardson, P. F.; Young, R.; Fajer, J. *Proc. Natl. Acad. Sci. U.S.A.* **1981**, *78*, 2652.
(13) Stolzenberg, A. M.; Strauss, S. H.; Holm, R. H. *J. Am. Chem. Soc.* **1981**, *103*, 4763.
(14) Barkigia, K. M.; Fajer, J.; Spaulding, L. D.; Williams, G. J. B. *J. Am. Chem. Soc.* **1981**, *103*, 176.
(15) Godwin, J. B.; Meyer, T. J. *Inorg. Chem.* **1971**, *10*, 2150.
(16) Bottomley, F.; Mukaida, M. *J. Chem. Soc., Dalton Trans.* **1982**, 1933.
(17) Armor, J. N.; Hoffman, M. Z. *Inorg. Chem.* **1975**, *14*, 444.
(18) Armor, J. *Inorg. Chem.* **1973**, *12*, 1959.
(19) Murphy, W. R., Jr.; Takeuchi, K. J.; Meyer, T. J. *J. Am. Chem. Soc.* **1982**, *104*, 5817.
(20) Murphy, W. R., Jr.; Takeuchi, K.; Barley, M. H.; Meyer, T. J. *Inorg. Chem.* **1986**, *25*, 1041.
(21) Rhodes, M. R.; Meyer, T. J. *Inorg. Chem.* **1988**, *27*, 4772.
(22) Rhodes, M. R.; Barley, M. H.; Meyer, T. J. *Inorg. Chem.* **1991**, *30*, 629.
(23) Barley, M. H.; Takeuchi, K.; Murphy, W. R., Jr.; Meyer, T. J. *J. Chem. Soc., Chem. Commun.* **1985**, 507.
(24) Barley, M. H.; Takeuchi, K. J.; Meyer, T. J. *J. Am. Chem. Soc.* **1986**, *108*, 5876.
(25) Barley, M. H.; Rhodes, M. R.; Meyer, T. J. *Inorg. Chem.* **1987**, *26*, 1746.
(26) Toth, J. E.; Anson, F. C. *J. Am. Chem. Soc.* **1989**, *111*, 2444.
(27) Spence, J. T. In *Metal Ions in Biological Systems*; Sigel, H., Ed.; Marcel Dekker: New York, 1976; Vol. 5, Chapter 6.
(28) Felton, R. H. In *The Porphyrins, Part C*; Dolphin, D., Ed.; Academic Press: New York, 1978; Vol. 5, p 53.
(29) Dong, S.; Jiang, R. *J. Inorg. Biochem.* **1987**, *30*, 189.
(30) Macor, K. A.; Spiro, T. G. *J. Am. Chem. Soc.* **1983**, *105*, 5601.

0020-1669/92/1331-3280$03.00/0

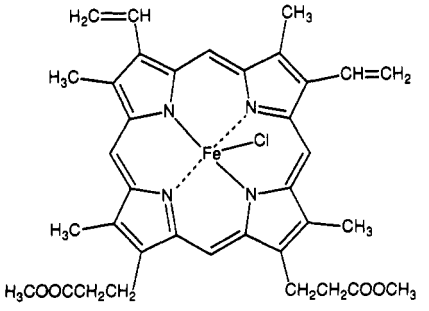

1

Figure 1. Structure of chloroiron(III) protoporphyrin IX dimethyl ester, $Fe^{III}(PP)Cl$.

Experimental Section

Materials. Tetra-*n*-butylammonium hexafluorophosphate (TBAH) for nonaqueous electrochemistry was supplied by Aldrich and was recrystallized twice from ethanol and then precipitated into ether from acetonitrile. The free-base porphyrin, protoporphyrin IX dimethyl ester (H_2PP), was purchased from Porphyrin Products (Logan, UT) and metalated with $FeCl_2$ in DMF at 100 °C by a standard procedure.[31]

Methylene chloride (Burdick and Jackson) and 1,2-difluorobenzene (Aldrich) were passed through a 1-in. plug of activated alumina prior to electrochemical measurements. Locally distilled, deionized water was utilized in all aqueous experiments. Buffered media (pH > 2) consisted of 0.1 M solutions of phosphate mixtures (H_3PO_4, KH_2PO_4, Na_2HPO_4) prepared from reagents supplied by Fisher Scientific and used without further purification. Solutions of pH < 2 were prepared 0.1 M in H_2SO_4/$NaHSO_4$ mixtures. Controlled-potential electrolyses were conducted at pH 2.1 in aqueous solutions 0.5 M in H_3PO_4 (ACS grade, Allied) and 0.25 M in tetraethylammonium hydroxide (60 wt % solution, Aldrich).

Electrochemical Techniques. Electrochemical measurements were obtained by using an EG&G Princeton Applied Research (PAR) Model 173 potentiostat/galvanostat equipped with a Model 179 digital coulometer. Excitation wave forms for cyclic voltammetric measurements were programmed with a PAR Model 175 universal programmer. Current–voltage curves or current–time curves were plotted on a Hewlett-Packard Model 7015B x-y recorder.

Electrochemical cells for cyclic voltammetric experiments were one-compartment glass containers equipped with Teflon tops to limit the access of air to the solution. The working electrode was a Teflon-shrouded glassy-carbon disk (0.1 cm^2) modified with a thin, electropolymerized metalloporphyrin film prepared as described below. A saturated sodium calomel electrode (SSCE) and a platinum coil were utilized as the reference and auxiliary electrodes, respectively. The aqueous buffered solutions were thoroughly deaerated and kept under a positive pressure of Ar during each run.

Controlled-potential electrolyses were conducted in a gastight cell connected to a mercury manometer to monitor gas production and allow for pressure equalization during each run. Two additional inlets sealed with straight-bore, ground-glass stopcocks permitted Ar purging prior to the electrolyses and sampling of the gaseous atmosphere during the runs. The modified vitreous carbon working electrode, platinum counter electrode, and sodium saturated calomel reference electrode were suspended from a threaded Teflon top into the stirred KNO_2 solution. A Vycor-tipped glass tube enclosed the auxiliary electrode, providing separate anodic and cathodic compartments within the cell. All openings of the top were sealed with O-rings, and gas leakage from the cell was determined to be minimal over a 4-h period. In a typical electrolysis experiment, 35 mL of pH 2.1 phosphate buffer was used. Nitrite ion was added as a 500-μL aliquot of a 0.1 M KNO_2 stock solution prepared by dissolving 85 mg of the reagent in 10 mL of H_2O.

Methods of Product Analysis. The products of catalysis were assayed by a combination of gas and liquid chromatographic separation techniques. Gas samples taken from the electrolysis cell with a Hamilton 100- or 500-μL gastight syringe were injected immediately into a Hewlett-Packard 5890A gas chromatograph equipped with a thermal conductivity detector for quantitative determination of N_2 and N_2O. Analysis of N_2 was conducted on an Alltech molecular sieve column (80/100 mesh) operated at 30 °C, 25 psi, using air as an external standard.[32] The numbers obtained were corrected for the N_2 residing in the cell prior to electrolysis. The amount of N_2O present was determined by using an Alltech Porapak Q column (80/100 mesh) which was standardized with carbon dioxide.[33] The analyses were conducted at 40 °C, 25 psi, and were corrected for the solubility of N_2O in aqueous solution.[34]

The remaining electrolysis products (NH_3, NH_2OH, N_2H_4) were analyzed as their monocations in acidic solution by using a Dionex 2000i ion-exchange chromatograph equipped with a conductivity detector and a HPIC-CS2 column. Samples for chromatographic analysis were prepared by diluting 10 mL of the electrolyzed solution to 19.5 mL and adding HPF_6 (~0.2 mL) to give a pH of 1.5 as determined with pH paper. The acidified solution was suction filtered two times without washings into a dry filter flask to remove the excess precipitated NEt_4PF_6. The filtrate was injected into the ion chromatograph and analyzed at a flow rate of 1 mL/min by using an aqueous eluent containing 3.0×10^{-2} M H_3PO_4 and 3.0×10^{-5} M $CuSO_4$. Under these experimental conditions, the ions eluted from the column in the order $Na^+ < NH_3OH^+ < NH_4^+ < K^+ < N_2H_5^+ < NEt_4^+$.

Preparation of Metalloporphyrin-Modified Electrodes. Films of electropolymerized $Fe^{III}(PP)Cl$ were deposited on freshly polished (1-μm Buehler diamond paste) glassy-carbon electrodes or optically transparent SnO_2 electrodes (Delta Technologies, Inc.) by immersing the electrode in an argon-blanketed dichloromethane solution 1.0 mM in the metalloporphyrin monomer and cycling the electrode potential repeatedly between 0.00 and +1.30 V vs SSCE. This procedure was analogous to that described by Dong and Jiang[29] and Macor and Spiro.[30] After approximately 15 scans, further growth of the polymeric film was limited. Alternatively, films were deposited by holding the potential of the electrode past or within the porphyrin-based oxidation at $E_{p,a}$ = +1.20 V for 15 min. Following the electropolymerization step, the coated electrodes were rinsed thoroughly with pure solvent. The quantity of electroactive porphyrin on the modified electrodes, Γ in mol/cm^2, was determined by integration of the peak area under a cathodic Fe^{III}/Fe^{II} cyclic voltammetric wave obtained by scanning a metalloporphyrin-modified electrode in electrolyte solution containing no external monomer. For glassy-carbon electrodes (0.1 cm^2), average coverages of 5.5×10^{-9} mol/cm^2 were obtained by repeated cycling between 0.00 and +1.30 V. Assuming that the porphyrin units lay flat on the electrode surface, each occupying an area of 144 Å^2, approximately 1.2×10^{-10} mol/cm^2 comprised one monolayer.[35] Thus, about 45 monolayers were deposited on the modified electrode surface. Somewhat heavier coverages ($(8–9) \times 10^{-9}$ mol/cm^2) were observed by potentiostating the electrode within the oxidative wave at $E_{p,a}$ = 1.20 V for 15 min.

Working electrodes for bulk electrolyses were cut to dimensions of approximately 0.5 cm × 0.5 cm × 2.5 cm from a vitrous carbon block containing 20 pores/in. These high-surface area electrodes were modified in a similar manner in an inert atmosphere (drybox) utilizing 1,2-difluorobenzene/0.1 M TBAH solutions containing the monomeric metalloporphyrin. (Adequate coverages of these electrodes were difficult to achieve using degassed CH_2Cl_2 as the solvent for electropolymerization.) The vitreous carbon electrodes contained approximately 550 times the modified surface coverage of the analytical electrodes.

Results

Solution Electrochemistry. A cyclic voltammogram of the porphyrin monomer in CH_2Cl_2 obtained at a scan rate of 100 mV/s is shown in Figure 2a. The metal-based Fe^{III}/Fe^{II} reduction was observed at $E_{1/2}$ = –0.42 V vs SSCE (sodium saturated calomel electrode). It displayed considerable peak splitting (~150 mV) at this scan rate consistent with slow, heterogeneous charge transfer. Sweeping further in the cathodic direction gave rise to a second, quasi-reversible reduction at –1.33 V vs SSCE, identified as a metal-centered Fe^{II}/Fe^{I} couple in previous electrochemical

(31) Adler, A. D.; Longo, F. R.; Kampas, F.; Kim, J. *J. Inorg. Nucl. Chem.* **1970**, *32*, 2443.

(32) Cowper, C. J.; DeRose, A. J. *Analysis of Gases by Chromatography*; Pergamon Press: Oxford, England, 1983; Vol. 7, p 83.

(33) Thompson, B. *Fundamentals of Gas Analysis by Gas Chromatography*; Varian: Palo Alto, CA, 1977; p 22.

(34) *Handbook of Chemistry and Physics*, 55th ed.; Weast, R. C., Ed.; CRC Press: Cleveland, OH, 1974; p B-115.

(35) Rocklin, R. D.; Murray, R. W. *J. Electroanal. Chem. Interfacial Electrochem.* **1979**, *100*, 271.

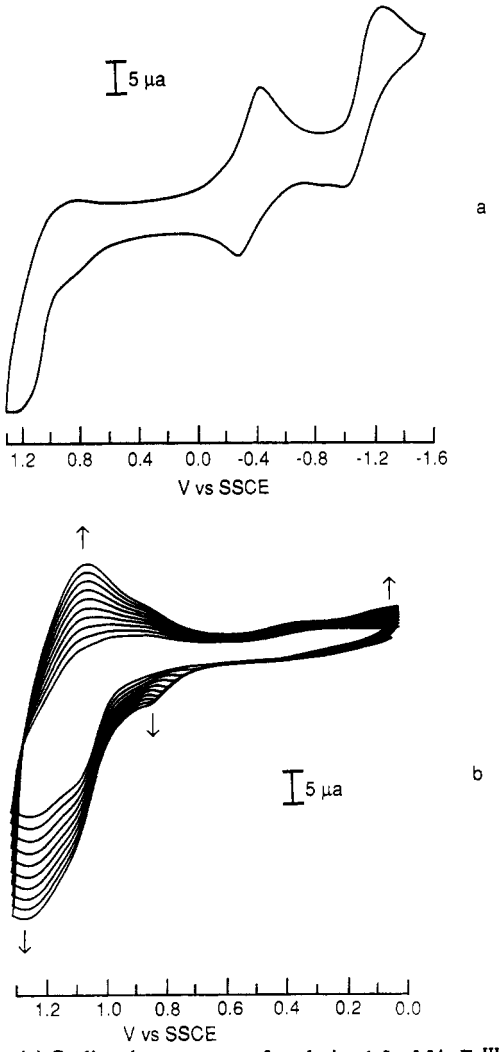

Figure 2. (a) Cyclic voltammogram of a solution 1.5 mM in $Fe^{III}(PP)Cl$ in 0.1 M $TBAH/CH_2Cl_2$ at a glassy-carbon electrode (100 mV/s). (b) Consecutive cyclic voltammetric scans as in (a) but in a solution 1 mM in $Fe^{III}(PP)Cl$, demonstrating the growth of a conductive film on the electrode surface.

studies.[28,36] Spectroscopic properties[37] corroborate this assignment: Electrochemical reduction of iron(II) tetraphenylporphyrin, $Fe^{II}(TPP)$, at the second wave yields a complex consistent with a low-spin d^7 $Fe^{I}(TPP)^-$ complex rather than the Fe^{II} porphyrin π-anion. The anodic cyclic voltammogram of $Fe^{III}(PP)Cl$ showed an irreversible wave at $E_{p,a} = 1.19$ V vs SSCE assigned to ring oxidation to the cation radical as observed in related systems.[38-42]

Electropolymerization of $Fe^{III}(PP)Cl$. Successive increases in the oxidative and reductive peak currents were observed during repeated cycling (0.00–1.30 V vs SSCE) of glassy-carbon or optically transparent SnO_2 electrodes immersed in a CH_2Cl_2 solution containing $Fe^{III}(PP)Cl$ (Figure 2b). From the enhanced peak currents it could be inferred that an electroactive layer was deposited on the electrode surface which was capable of mediating

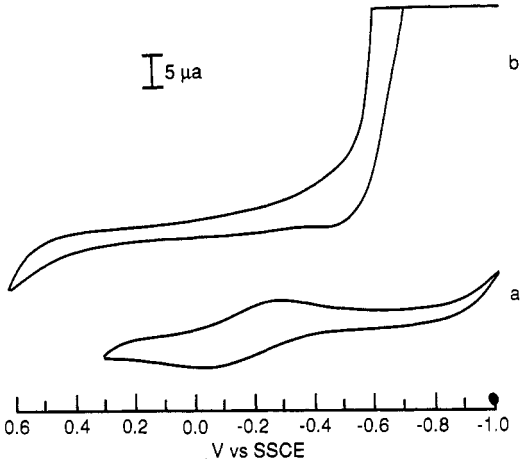

Figure 3. Cyclic voltammograms at an $Fe^{III}(PP)Cl$-modified electrode ($\Gamma = 5.5 \times 10^{-9}$ mol/cm^2) at 20 mV/s in (a) pH 2.49 phosphate buffer and (b) pH 2.49 phosphate buffer containing 0.01 M $NaNO_2$.

the electrolysis of incoming porphyrin monomer at the film-solution interface. The surface coverages increased steadily through approximately 15 scans after which further growth was limited. As the thickness of the polymeric film increased, electron migration through the layer was probably slowed, limiting the rate of polymerization of the metalloporphyin monomer. Following thorough washing with CH_2Cl_2 to remove excess adsorbed monomer, a deeply colored coating was visually apparent on the electrode surface. The films adhered strongly to the electrode surface and were stable to rinsing with aqueous or organic (CH_3CN, CH_2Cl_2, Me_2CO) solvents. Attempts to prepare modified electrodes by cycling reductively between 0.00 and −1.60 V were unsuccessful in CH_2Cl_2, DMF, or CH_3CN. However, the porphyrin underwent slow reductive electropolymerization from solutions of 1,2-difluorobenzene in an inert atmosphere.[43]

The cyclic voltammogram shown in Figure 3a was measured at the film-modified electrode immersed in a $H_3PO_4/H_2PO_4^-$ buffer solution at pH 2.49 containing no external porphyrin monomer. In the voltammogram, the reductive and oxidative waves of the $Fe^{III/II}$ couple appeared at $E_{p,c} = -0.25$ and $E_{p,a} = -0.05$ V vs SSCE, respectively, at a scan rate of 20 mV/s. Compared to the $Fe^{III/II}$ couple of the porphyrin monomer in CH_2Cl_2 (Figure 2a), the Fe^{III}/Fe^{II} reduction in the polymeric film was shifted anodically, and there was an increased peak-to-peak splitting ($\Delta E_p = 200$ mV) consistent with slow, heterogeneous charge transfer between the electrode and the redox centers in the polymeric film. The peak-to-peak splitting increased with increasing scan rate confirming the quasi-reversible nature of the Fe^{III}/Fe^{II} reduction. At a scan rate of 200 mV/s, the observed ΔE_p was 310 mV ($E_{p,c} = -0.29$ and $E_{p,a} = +0.02$ V vs SSCE). The films were stable to 30 cycles at negative potentials encompassing only the first reductive wave (i.e., 0.00 to −1.00 V vs SSCE). A single cathodic scan into the second reduction at −1.33 V rendered the electrode nonconductive, although a deeply colored film was still visible on the electrode surface. The film was also unstable toward oxidative scanning: One cycle between 0.00 and +1.30 V vs SSCE resulted in an electroinactive polymeric film.

As seen in Figure 4, there was considerable similarity between the UV/visible spectrum of a CH_2Cl_2 solution of monomeric $Fe^{III}(PP)Cl$ and that of the metalloporphyrin film deposited on an optically transparent SnO_2 electrode. Despite the increased background absorption resulting from light scattering, it was evident that the porphyrin macrocycle was maintained during the electrodeposition, consistent with bond formation at the peripheral vinyl groups in the polymerization step. The four

(36) Bond, A. M.; Mann, T. F.; Tondreau, G. A.; Sweigart, D. A. *Inorg. Chim. Acta* **1990**, *169*, 181.
(37) Hickman, D. L.; Shirazi, A.; Goff, H. M. *Inorg. Chem.* **1985**, *24*, 563.
(38) English, D. R.; Hendrickson, D. N.; Suslick, K. S. *Inorg. Chem.* **1983**, *22*, 367.
(39) Buisson, G.; Deronzier, A.; Duee, E.; Gans, P.; Marchon, J.-C.; Regnard, J.-R. *J. Am. Chem. Soc.* **1982**, *104*, 6793.
(40) Scholz, W. F.; Reed, C. A.; Lee, Y. J.; Scheidt, W. R.; Lang, G. *J. Am. Chem. Soc.* **1982**, *104*, 6791.
(41) Shimomura, E. T.; Phillippi, M. A.; Goff, H. M.; Scholz, W. F.; Reed, C. A. *J. Am. Chem. Soc.* **1981**, *103*, 6778.
(42) Phillippi, M. A.; Shimomura, E. T.; Goff, H. M. *Inorg. Chem.* **1981**, *20*, 1322.
(43) O'Toole, T. R.; Younathan, J. N.; Sullivan, B. P.; Meyer, T. J. *Inorg. Chem.* **1989**, *28*, 3923.

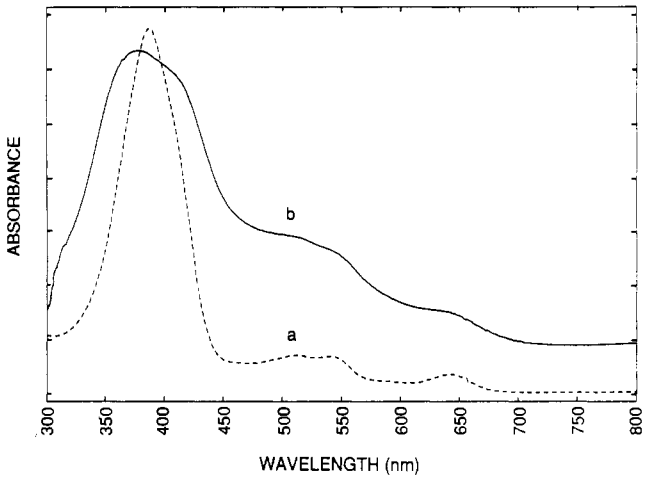

Figure 4. Absorption spectra of (a) 1.5×10^{-5} M $Fe^{III}(PP)Cl$ in CH_2Cl_2 and (b) a polymeric $Fe^{III}(PP)Cl$ film on a transparent SnO_2 electrode immersed in CH_2Cl_2, $\Gamma = 9 \times 10^{-9}$ mol/cm^2. The scale of the vertical axis is enlarged (×4.5) for spectrum b.

bands associated with the strong B (Soret) absorption and weaker Q_1 and Q_0 $\pi \rightarrow \pi^*$ transitions of the porphyrin heterocycle[44] were evident in both the film and solution spectra. The broad absorption bands reflect the heterogeneity of the chromophoric sites, perhaps arising from varying orientations, mixed peripheral vinyl substitution, and porphyrin–porphyrin interactions within the polymer. On the basis of the absorbance of the modified SnO_2 electrode at 510 nm and the known solution extinction coefficient for $Fe^{III}(PP)Cl$ in CH_2Cl_2, a surface coverage Γ of 9×10^{-9} mol/cm^2 was calculated.[45] This coverage corresponded to approximately 75 monolayers on the electrode surface (see Experimental Section).

Evidence for Catalysis. The cathodic cyclic voltammogram of an aqueous solution containing $NaNO_2$ at pH 2.49 (Figure 3b) showed a current enhancement at a modified electrode that was not observed in the absence of the metalloporphyrin film. Scans at an $Fe^{III}(PP)Cl$-modified electrode (0.1 cm^2, $\Gamma = 5.5 \times 10^{-9}$ mol/cm^2) in the presence of 10^{-2} M $NaNO_2$ resulted in a large catalytic wave at potentials more negative than –0.50 V vs SSCE with catalytic currents as high as 337 μA at –0.68 V. By comparison, a maximum current of 10.8 μA was observed under identical conditions at an untreated glassy-carbon electrode. Furthermore, the current response at the film-coated electrode was dependent on the amount of NO_2^- present as evidenced by the data in Figure 5. The current–potential profile past –0.50 V was a featureless wave with $E_{p,c} = -0.68$ V at pH 2.49 (Figure 5).

Electrochemistry in the Presence of Nitrite. Upon addition of nitrite (6×10^{-4}–10^{-2} M) to an aqueous buffer solution at pH 2.49, the metal-centered $Fe^{III/II}$ wave disappeared from the voltammogram (Figures 3b and 5). Under these conditions (pH < 4), free NO is generated in solution from the disproportionation of nitrous acid.[46-48] Although disproportionation is relatively slow under our conditions, there is a relatively small amount of porphyrin on the electrode surfaces.[48]

$$3HONO \rightarrow H^+ + NO_3^- + 2NO + H_2O \qquad (2)$$

Once formed, NO can react directly with $Fe^{III}(PP)Cl$ yielding the porphyin nitrosyl complex **2**. Disproportionation even to a limited extent is sufficient to drive this reaction to completion, suggesting a high affinity of $[Fe^{III}(PP)]^+$ for NO. The state of axial ligation trans to NO is unknown.

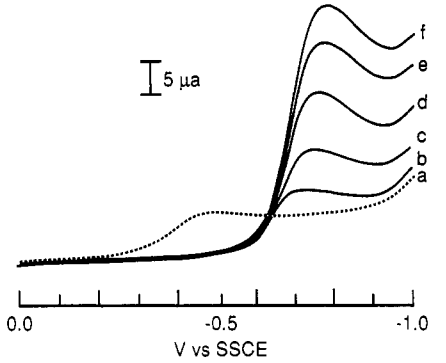

Figure 5. Linear sweep voltammograms at an $Fe^{III}(PP)Cl$-modified electrode ($\Gamma = 5.5 \times 10^{-9}$ mol/cm^2) immersed in pH 2.49 phosphate buffer containing $NaNO_2$ in concentrations of (a) 0.0 M, (b) 6.48×10^{-4} M, (c) 1.18×10^{-3} M, (d) 2.18×10^{-3} M, (e) 3.02×10^{-3} M, and (f) 4.22×10^{-3} M. The scan rate was 20 mV/s.

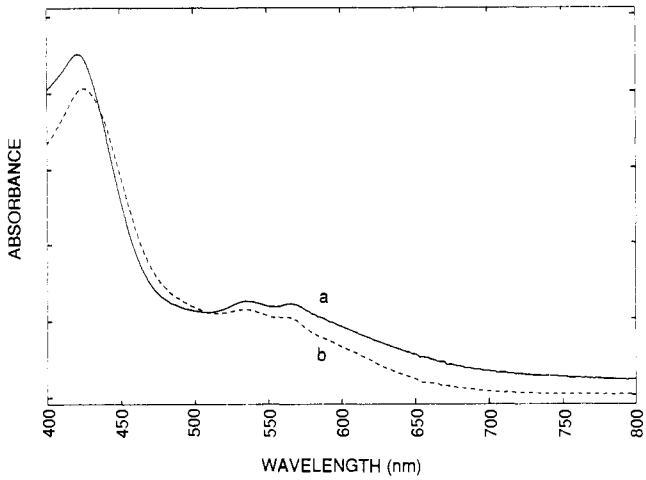

Figure 6. Absorption spectra of an $Fe^{III}(PP)Cl$ film on an optically transparent SnO_2 electrode in pH 2.49 buffer solution (a) containing 0.06 M $NaNO_2$ and (b) saturated with NO gas.

$$\underset{\mathbf{1}}{[Fe^{III}(PP)]^+} + NO \rightarrow \underset{\mathbf{2}}{[Fe^{II}(NO^+)(PP)]^+} \qquad (3)$$

The formation of the nitrosyl complex was supported by UV/visible spectral changes observed at film-coated, optically transparent electrodes. Figure 6a shows the absorption spectrum measured after immersing an $Fe^{III}(PP)Cl$-modified electrode in an argon-purged, buffered (pH 2.49) solution containing 0.06 M nitrite for 15 min. A nearly identical absorption spectrum (Figure 6b) was observed at a modified electrode immersed in an aqueous, acidic solution saturated with NO gas, confirming the initial formation of nitrosyl complex **2**. In addition, the observed absorption maxima in Figure 6a (424, 536, 564 nm) resembled those reported for an aqueous solution of $[Fe^{II}(NO^+)(TPPS)]^{3-}$ [TPPS = *meso*-tetrakis(*p*-sulfonatophenyl)porphyrin sexianion] at 425, 540, and 576 nm.[24] Aqueous solutions of **2** were unstable in air presumably because NO is removed from the system by oxidation to NO_2.

(44) Gouterman, M. In *The Porphyrins, Part A*; Dolphin, D., Ed.; Academic Press: New York, 1978; Vol. 3, p 1.

(45) The surface coverage, Γ, in mol/cm^2 is related to the optical density, A, by the formula $A = \epsilon\Gamma \times 1000$ cm^3/L, where ϵ is the molar extinction coefficient in mol^{-1} cm^{-2}.

(46) Cotton, F. A.; Wilkinson, G. *Advanced Inorganic Chemistry*; 5th ed.; Wiley: New York, 1988; p 327.

(47) Stedman, G. *Adv. Inorg. Chem. Radiochem.* **1979**, *22*, 113.

(48) Nitrous acid (5 mM) undergoes disproportionation to give NO_3^- and NO in a second-order process with a half-life of ~2 h at pH 3.1 (Binstead, R. A.; Meyer, T. J. Unpublished results). Although the moles of NO produced by this reaction during a 10-min cyclic voltammetric experiment are small (approximately 3×10^{-6} mol in 2 mL of a 0.01 M $NaNO_2$ solution, pH 2.49), this amount greatly exceeds the moles of porphyrin catalyst on the electrode surface (5.5×10^{-10} mol on a typical modified analytical electrode). From our observations $[Fe^{III}(PP)]^+$ is converted quantitatively into $[Fe^{II}(NO^+)(PP)]^+$ under the conditions used, and the $[Fe^{III}(PP)]^+/[Fe^{II}(PP)]^0$ couple is not observed in the voltammograms.

Table I. Products of Electrocatalytic Reduction of Nitrite at an $Fe^{III}(PP)Cl$-Modified Electrode[a,b]

E_{app}, V vs SSCE	time, h	electrons per NO_2^-	current, mA[c] i_i	current, mA[c] i_f	electrons per $Fe^{III}(PP)Cl$	tot. charge Q_f, C	product distribution, %[d] N_2O	N_2	NH_2OH	N_2H_4	NH_3	current efficiency, %[e] N_2O	N_2	NH_2OH	N_2H_4	NH_3
−0.6	3.0	3.0	5.0	1.5	410	17.5	18	35	16	<1	31	10 ± 1	29 ± 2	18 ± 6	0	51 ± 5
−0.7	4.0	3.8	22.5	0.9	430	18.3	12	39	13	2	34	6	31	14	3 ± 1	54
−0.8	1.0	4.8	18.5	1.5	545	23.1	<1	30	13	<1	63	0	19	11	0	80
−0.9	2.5	5.8	8.0	3.2	660	28.0	<1	35	13	<1	52	0	18	9	0	54
−0.9[f]	7.5	5.2	100.0	0.2			8	<1	<1		84	3	0	0		97
−0.9[g]	4.0	3.3	61.0	1.0		16.1	32	14	13	<1	27	19	8	15	0	56

[a] The surface area of the modified electrode containing the film was 55 cm^2 with a surface coverage of 8×10^{-9} mol/cm^2. [b] All electrolyses were conducted with $[NO_2^-] = 1.4 \times 10^{-3}$ M at a pH of 2.1. [c] Initial (i_i) and final (i_f) current levels. [d] The product yields are expressed as a mole percentage of the NO_2^- present at the beginning of the electrolysis (5×10^{-5} mol). [e] The percent current efficiency for each of the products was calculated from the following formula: current efficiency (%) = $[(n_i n_i F)/Q_f]$ 100%. n_i is moles of product formed, n_i is the n value for its formation ($n = 4$ for N_2O, $n = 6$ for N_2, $n = 4$ for NH_2OH, $n = 10$ for N_2H_4, and $n = 6$ for NH_3), F is the Faraday constant, and Q_f is the total charge passed during the electrolysis. Typical uncertainties are given for the first electrolysis. [f] The catalyst was $[Fe^{III}(H_2O)(TPPS)]^{3-}$ [TPPS = *meso*-tetrakis(*p*-sulfonatophenyl)porphyrin sexianion]. [g] The catalyst was $[Fe^{III}(H_2O)(TMPyP)]^{5+}$ [TMPyP = *meso*-tetrakis(*N*-methyl-4-pyridiniumyl)porphyrin dication].

Differential pulse polarographic measurements of the nitrosyl complex of $[Fe^{III}(H_2O)(TPPS)]^{3-}$ show a one-electron reduction for the $[Fe^{II}(NO^+)TPPS]^{3-}/[Fe^{II}(NO^\bullet)TPPS]^{4-}$ couple at $E_{1/2}$ = +0.35 V vs SCE (pH 3.01).[24] The corresponding wave in the cyclic voltammogram is broad and ill-defined. Likewise, at an $Fe^{III}(PP)Cl$-modified electrode immersed in a buffered solution of 0.01 M nitrite, a well-defined reduction wave for the $[Fe^{II}(NO^+)(PP)]^+/[Fe^{II}(NO^\bullet)(PP)]^0$ couple was not observed in the cyclic voltammogram in cathodic scans from +0.50 to −1.00 V. However, when cyclic voltammetric sweeps were initiated at 0.00 V, a noticeable current flow was observed when the circuit was connected, while initiation of the sweeps at +0.50 V gave no evidence for prompt current flow. By analogy to the earlier studies, this current presumably resulted from one-electron reduction of nitrosyl complex **2** to generate **3**. In addition, the

$$\underset{\mathbf{2}}{[Fe^{II}(NO^+)(PP)]^+} \rightarrow \underset{\mathbf{3}}{[Fe^{II}(NO^\bullet)(PP)]^0} \qquad (4)$$

onset of the catalytic wave at the $Fe^{III}(PP)Cl$-modified electrode (Figure 3b) at ~−0.4 V showed a shoulder with a distinct return component at −0.5 V. This wave was assigned to the $[Fe^{II}(NO^\bullet)(PP)]^0/[Fe^{II}(NO^-)(PP)]^-$ couple by comparison with the solution electrochemistry of $[Fe^{III}(H_2O)(TMPyP)]^{5+}$ [TMPyP = *meso*-tetrakis(*N*-methyl-4-pyridiniumyl)porphyrin dication].[25] The $[Fe^{II}(NO^\bullet)(TMPyP)]^{4+}/[Fe^{II}(NO^-)(TMPyP)]^{3+}$ redox couple for this porphyrin occurs at $E_{p,c}$ = −0.63 V and $E_{p,a}$ = −0.45 V and is similar in appearance to the film-based wave. The catalytic waves for both complexes are clearly multielectron in nature, concealing individual steps in the further reduction of $[Fe^{II}(NO^-)(PP)]^-$ or $[Fe^{II}(NO^-)(TMPyP)]^{3+}$ within the broad envelope of the catalytic reduction wave.

Products of the Catalytic Reductions. The results of controlled-potential electrolyses at the metalloporphyrin-modified electrode are summarized in Table I both as the percent conversion to a given product and as the percentage of the current passed in forming a particular product. For comparison, the results of homogeneous catalytic reductions mediated by $[Fe^{III}(H_2O)(TMPyP)]^{5+}$ or $[Fe^{III}(H_2O)(TPPS)]^{3-}$ at −0.9 V are also included in Table I. In the absence of the film or solution porphyrin catalysts, the background current was negligible. The products of the electrolyses were analyzed when the current levels had dropped to approximately 10% of the initial value due to exhaustion of available NO_2^-. The major products of the catalytic reductions were ammonia, nitrous oxide, nitrogen, and hydroxylamine. In general, these products successfully accounted for all of the charge passed during the electrolysis, except for the experiment at −0.9 V, where the current efficiencies totaled 81%. We were unable to account for the remaining reductive equivalents at this potential although reduction of H^+ to H_2 is a possibility.

The most highly reduced product, NH_3, was favored as the electrolysis potential became more negative. The enhanced production of NH_3 came at the expense of the two-electron product, N_2O. By inference, the reaction sequence involves a twice-reduced intermediate, $[Fe^{II}(NO^-)(PP)]^-$, which partitions between the formation of N_2O and further reduction to form the six-electron reduction product NH_3. The effective n value or number of electrons added per NO_2^- increased by approximately 1 with each 100-mV increment in applied potential between −0.6 and −0.9 V.

Scheme I. Possible Mechanism for the Electrocatalytic Reduction of NO_2^- or NO

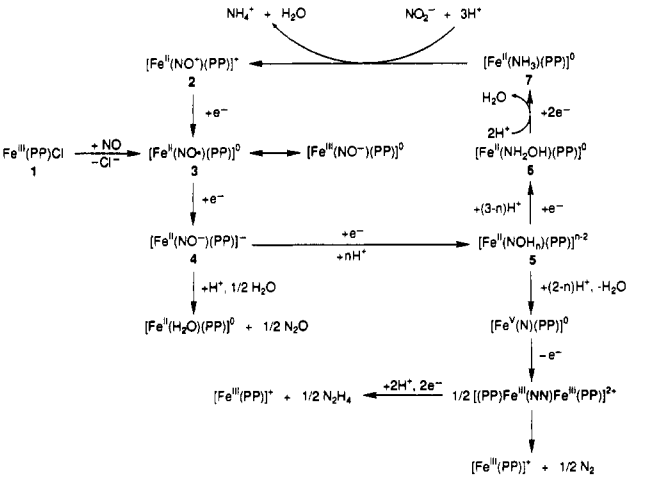

Discussion

Oxidative electropolymerization of $Fe^{III}(PP)Cl$ readily forms a conductive film on inert electrodes which catalyzes the electroreduction of NO or nitrite to ammonia, nitrous oxide, nitrogen, and hydroxylamine. Resonance Raman studies on related films prepared from $Ni^{II}(PP)$ indicate that, on average, one of the two vinyl groups in each porphyrin is saturated. Consequently, it has been suggested that a radical cationic polymerization of the peripheral vinyl groups is operative in the formation of the polymeric films.[30]

The polymeric films that result are chemically accessible to NO and possibly to small, charged ions such as NO_2^-, as evidenced by the loss of the Fe^{III}/Fe^{II} wave upon addition of 0.01 M nitrite to the external electrolyte solution. In general, the films become deactivated with an extended series of successive reductive scans or repeated bulk catalytic reductions. In one example, the initial current level at a previously used electrode was only 10% of that observed for the first bulk catalytic reduction. The electronic spectrum of the film does not change after exhaustive bulk electrolysis. After potentiostating at −0.8 V for 45 min, the absorption spectrum at a film-modified electrode in 0.06 M $NaNO_2$ was identical to the spectrum shown in Figure 6a taken prior to electrolysis.

A plausible mechanism for the reduction of NO_2^- in acidic solution is shown in Scheme I. This mechanism is based on the results of cyclic voltammetry and product analyses following controlled-potential electrolyses combined with previous solution studies on metalloporphyrin-catalyzed electrochemical reduction of nitrite.[21,23-25] Scheme I also shares certain steps in common with the interconversion of $M^{II}(NO^+)$ to $M^{II}(NH_3)$ in polypyridyl complexes of Ru^{II} and Os^{II}.[19-22,49] Spectral and electrochemical evidence support the formation of the nitrosyl complex, $[Fe^{II}(NO^+)(PP)]^+$, at the metalloporphyrin sites in the polymeric matrix. Following an initial nitrosyl-based reduction, a multielectron step occurs that rapidly forms the reduced products and returns the metalloporphyrin to the nitrosyl form. The two-electron product N_2O is produced via N–N coupling, perhaps involving a dimerization as in eq 5. The N–N coupling step to yield N_2O must be in competition with further reduction of the NO^- ligand, since, at increasingly negative potentials, the yield of NH_3 increases at the expense of N_2O.

$$2[Fe^{II}(NO^-)(PP)]^- + H_2O + 2H^+ \xrightarrow[4]{} 2[Fe^{II}(H_2O)(PP)]^0 + N_2O \quad (5)$$

The presence of significant amounts of both N_2 and hydroxylamine suggests that the hydrated three-electron product $[Fe^{II}(NOH_n)(PP)]^{n-2}$ can eliminate water in competition with reduction to $[Fe^{II}(NH_2OH)(PP)]^0$, possibly leading to a nitrido complex and, ultimately, to the formation of N_2. The formation of N_2 as a major product from metalloporphyrin-mediated nitrite reduction is the most striking difference between the heterogeneous system and the previously studied solution-phase monomeric porphyrin catalysts.[23-25] Under comparable conditions, nitrite reduction catalyzed by $[Fe^{III}(H_2O)(TPPS)]^{3-}$ or $[Fe^{III}(H_2O)(TMPyP)]^{5+}$ yields <1% or 14% N_2, respectively, while electroreduction with the film-modified electrodes yields 35%–39% N_2 depending on the applied potential. (See Table I.) The enhanced N–N coupling observed with the film catalyst may be a consequence of the enforced spatial proximity between the redox sites within the polymeric matrix. Likewise, a rhenium(I) catalyst for CO_2 reduction yields the C–C coupled product oxalate anion when electrodeposited as a thin polymeric film on an electrode surface but not as a monomeric catalyst in homogeneous solution.[50]

The sensitivity of the metalloporphyrin polymeric electrodes to millimolar quantities of $HONO/NO_2^-$ and NO suggests the possibility of using these or other modified electrodes as an analytical tool either by electrochemical measurements or by spectral measurements on optically transparent electrodes. The film-modified electrode is particularly sensitive to the presence of NO given its demonstrated affinity for the Fe^{III} porphyrin sites within the redox polymer even at low levels in the external solution.

Acknowledgment. Financial support from the National Institutes of Health (Grant No. 5-RO1-GM32296-08), the Army Research office, Durham, NC (Grant No. DAAL03-88-K-0192), and an NIH Postdoctoral Fellowship (No. 1-F32-GM11280-01A1) to J.N.Y. is gratefully acknowledged.

Registry No. 1, 15741-03-4; TBAH, 3109-63-5; $(Fe^{III}(PP)Cl)_n$, 140657-23-4; C, 7440-44-0; SnO_2, 18282-10-5; NO_2^-, 14797-65-0; NO, 14452-93-8; N_2O, 10024-97-2; N_2, 7727-37-9; NH_2OH, 7803-49-8; N_2H_4, 302-01-2; NH_3, 7664-41-7; HONO, 7782-77-6; $[Fe^{III}(H_2O)(TPPS)]^{3-}$, 53194-20-0; $[Fe^{III}(H_2O)(TMPyP)]^{5+}$, 65774-47-2; $NaNO_2$, 7632-00-0.

(49) Thompson, M. S.; Meyer, T. J. *J. Am. Chem. Soc.* **1981**, *103*, 5577.

(50) O'Toole, T. R.; Sullivan, B. P.; Bruce, M. R.-M.; Margerum, L. D.; Murray, R. W.; Meyer, T. J. *J. Electroanal. Chem. Interfacial Electrochem.* **1989**, *259*, 217.